AD_____

Award Number: **DAMD17-99-1-9335**

TITLE: **"Imaging of Early-Stage Breast Cancers Using Pulsed Confocal Microwave Technology"**

PRINCIPAL INVESTIGATOR: **Milica Popovic, M.Sc.**
Allen Taflove, Ph.D.

CONTRACTING ORGANIZATION: **Northwestern University**
Evanston, Illinois 60208-1110

REPORT DATE: **May 2001**

TYPE OF REPORT: **Annual Summary**

PREPARED FOR: **U.S. Army Medical Research and Materiel Command**
Fort Detrick, Maryland 21702-5012

REPORT DOCUMENTATION PAGE

Form Approved
OMB No. 074-0188

1. AGENCY USE ONLY (Leave blank)	2. REPORT DATE	3. REPORT TYPE AND DATES COVERED
	May 2001	Annual Summary (1 May 2000 - 30 April 2001)

4. TITLE AND SUBTITLE
Imaging of Early-Stage Breast Cancers Using Pulsed Confocal Microwave Technology

5. FUNDING NUMBERS
DAMD17-99-1-9335

6. AUTHOR(S)
Milica Popovic, M.Sc.
Prof. Allen Taflove, Ph.D.

7. PERFORMING ORGANIZATION NAME(S) AND ADDRESS(ES)
Northwestern University

Evanston, Illinois 60208- **1110**
E-Mail:
poppy@northwestern.edu

8. PERFORMING ORGANIZATION REPORT NUMBER

9. SPONSORING / MONITORING AGENCY NAME(S) AND ADDRESS(ES)
U.S. Army Medical Research and Materiel Command
Fort Detrick, Maryland 21702-5012

10. SPONSORING / MONITORING AGENCY REPORT NUMBER

11. SUPPLEMENTARY NOTES
This report contains colored photos

12a. DISTRIBUTION / AVAILABILITY STATEMENT
Approved for Public Release; Distribution Unlimited

12b. DISTRIBUTION CODE

13. ABSTRACT ***(Maximum 200 Words)***
We continue to investigate low-power confocal microwave technology to detect and image early-stage breast cancers. The technology exploits the dielectric property contrast between normal breast tissues and malignant tumors at microwave frequencies. The microwave imaging is performed by a planar antenna array contacting only one side of the breast. The antenna array elements collect backscattered signals. The digital signal processing scheme used for coherent summation of these signals depends upon the average dielectric properties of the local breast tissues. Patient-specific calibration of the microwave imager requires knowledge of these properties. To this end, this report summarizes continuing development of a two-dimensional time-domain inverse-scattering algorithm that allows for a noninvasive determination of the required dielectric properties of the near-surface breast layers. A method to sequentially determine properties of the breast skin, skin thickness and then the properties of the underlying breast tissue is suggested and investigated within a two-dimensional model.

14. SUBJECT TERMS
Breast cancer, Inverse-Scattering, Finite Difference Time Domain (FDTD), Microwave detection, Skin electrical properties

15. NUMBER OF PAGES
17

16. PRICE CODE

17. SECURITY CLASSIFICATION OF REPORT	18. SECURITY CLASSIFICATION OF THIS PAGE	19. SECURITY CLASSIFICATION OF ABSTRACT	20. LIMITATION OF ABSTRACT
Unclassified	Unclassified	Unclassified	Unlimited

NSN 7540-01-280-5500

Standard Form 298 (Rev. 2-89)
Prescribed by ANSI Std. Z39-18
298-102

Table of Contents

1. Introduction

We continue to investigate low-power confocal microwave technology to detect and image early-stage breast cancers. The technology exploits the dielectric property contrast between normal breast tissues and malignant tumors at microwave frequencies. The microwave imaging is performed by a planar antenna array contacting only one side of the breast. The antenna array elements collect backscattered signals. The digital signal processing scheme used for coherent summation of these signals depends upon the average dielectric properties of the local breast tissues. Patient-specific calibration of the microwave imager requires knowledge of these properties.

We are investigating a time-domain inverse-scattering technique to measure the skin thickness and dielectric parameters in the area of the human breast. Our study is motivated by several well-documented findings. Skin thickness is patient-specific, but we also note that within a single patient measurements revealed regional anatomical variations. A number of factors can cause thickening of mammary skin. Although our study is primarily motivated by assisting patient-specific calibration of the microwave breast cancer imaging system, we note that determining breast skin thickness can also help diagnose possible pathologies in the underlying tissue and in the patient in general.

In this report, we illustrate by simple calculation the importance of correct skin thickness assumption for calculating time delays essential for the image-formation signal processing algorithm of the microwave system. Furthermore, we present results of development of the two-dimensional time-domain inverse-scattering algorithm for simultaneous estimate of electrical permittivity $\varepsilon_{r\text{-}skin}$ and conductivity σ_{skin} of the skin layer. This algorithm locates the search trajectory in the ($\varepsilon_{r\text{-}skin}$, σ_{skin}) space. The minimal parameter estimation error along this trajectory should yield a set of correct parameter values.

Our investigations show that the search trajectory and the convergence error depend on the shape and the duration of the pulse chosen for the electrical parameter reconstruction. The time-domain nature of the inverse-algorithm allows for limiting the region of inversion. Thus, when the parameters of skin are estimated, the skin thickness can be determined by comparing the measurement with a simulated all-skin response. After this step, the skin thickness, $\varepsilon_{r\text{-}skin}$ and σ_{skin} are known, and, by exploiting the causality principle, we can employ the same inversion scheme to determine the electrical parameters of the underlying breast fatty tissue. Current and near-future work involves testing the algorithm robustness in the presence of Gaussian noise for various signal-to-noise ratios.

2. Body

2.1 Skin thickness in the area of the human breast

Breast skin thickness can be estimated from film-screen mammograms [3]. Skin thickness is patient-specific, but we also note that within a single patient measurements revealed regional anatomical variations [3], [6]-[15]. From the mediolateral view, the range in skin thickness in the superior breast area is 0.7-2.3mm, and in the inferior area 0.7-2.7mm. From the craniocaudad view, skin thickness ranges 0.6-2.4mm and 0.5-2.1mm in the medial and lateral area,

respectively. A number of factors can cause thickening of mammary skin [3], [6]-[15]. The major reported localized causes are carcinoma, inflammation, trauma, fat necrosis, post-biopsy and dermatological conditions. Among the generalized factors associated with increase in breast skin thickness are breast cancer, metastatic disease, inflammation, primary skin disorders, anasarca, any cause of lymphatic obstruction, radiation therapy and surgery. Although our study is primarily motivated by assisting patient-specific calibration of the microwave breast cancer imaging system of [1,2], we note that determining breast skin thickness can also help diagnose possible pathologies in the underlying tissue and in the patient in general.

2.2 Microwave breast tumor imaging system: dependency on the correct skin thickness

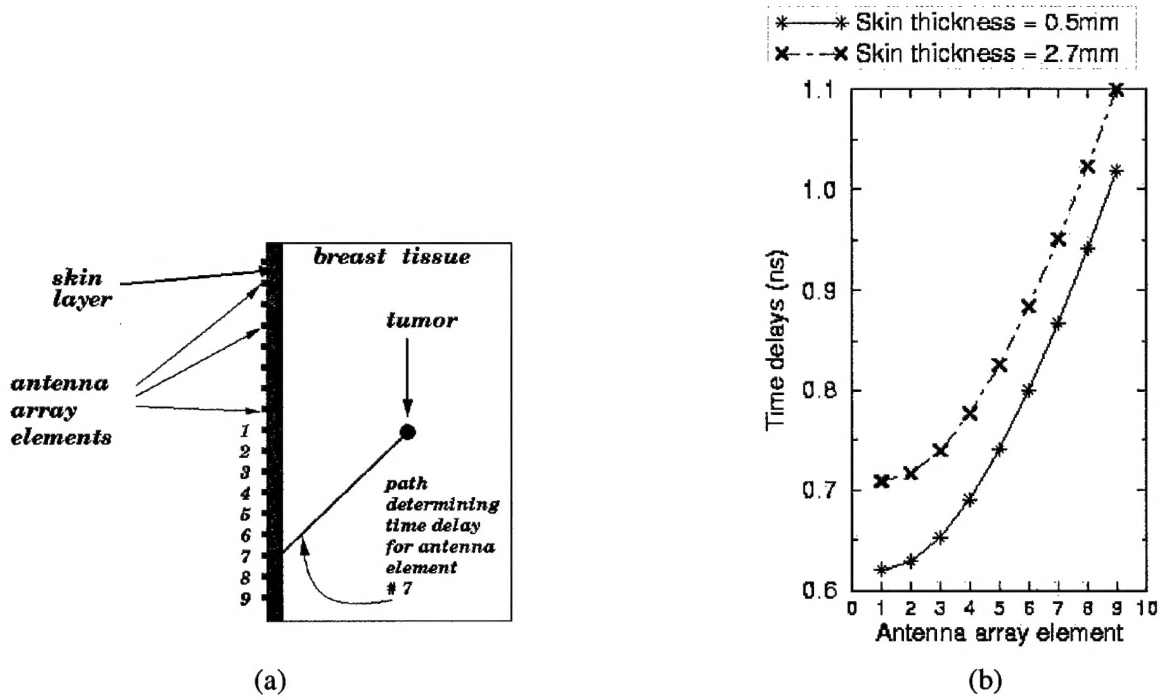

Figure 1. (a) 2-D sketch of the microwave antenna array used for breast tumor detection. The sketch shows the propagation path used to determine time delay between transmission and reception of the signal backscattered from the tumor for each antenna element. (b) Analytically calculated time delays for antenna array elements for extreme values of the reported breast skin thickness range.

To illustrate the importance of knowledge of correct skin thickness value on the operation of the microwave tumor imaging system of [1] in Fig. 1(a) we sketch a simplified 2-D geometry of a 17-element microwave antenna array system adjacent to the breast skin. Beneath the skin is a homogeneous slab of the fatty breast tissue. We assume the tumor location to be on the antenna array axis and 3 cm deep in the breast tissue. The system relies on high dielectric contrast between tumors and the healthy tissue in the microwave frequency range (relative electric permittivity: tumor $\varepsilon_{r\text{-}tumor} = 50$, breast tissue $\varepsilon_{r\text{-}breast} = 9$, skin $\varepsilon_{r\text{-}skin} = 36$, electric conductivity: tumor $\sigma_{tumor} = 7$ S/m, breast tissue $\sigma_{breast} = 0.4$ S/m, skin $\sigma_{skin} = 4$ S/m) [1]. A sub-nanosecond pulse is launched from each array element, which then collects the reflection. For each element, there is a time delay between the pulse transmission and its received reflection. This delay is

determined by a propagation path illustrated in Fig. 1(a), and calculated with assumed knowledge of skin thickness and dielectric parameters of skin and breast tissue – all media present in the propagation path. As a signal processing stage, the difference in time delays for different array elements is used to shift and coherently sum signals received by individual elements, thus achieving signal gain through this coherent summation. Therefore, an incorrect assumption of skin thickness and/or $\varepsilon_{r\text{-}skin}$ can cause incorrect calculation of time delays and hence lack of coherency in summation of signals received by different antenna array elements.

Fig. 1(b) graphs the calculated time delays as a function of antenna element location for the extreme values of the breast skin thickness range. We see that the variation in these delays for two skin thickness values is comparable to the difference in time delays for two adjacent antennas for each thickness value under consideration. We conclude that the knowledge of the correct value for skin thickness at each point of the imaged breast area is essential for efficient operation of the newly proposed microwave breast cancer detection system.

2.3 Obtaining the skin thickness

Before describing results for the algorithm for simultaneous recovery of both skin electrical parameters, we here briefly illustrate how we can proceed in estimating the breast skin thickness once the patient-specific values for $\varepsilon_{r\text{-}skin}$ and σ_{skin} are determined, as illustrated with FDTD simulation results in Fig. 2 for an assumed 60-ps differentiated Gaussian pulse. Due to the dielectric contrast between skin and the underlying breast tissue, the propagating pulse reflects off the skin – breast tissue interface. By comparing the response for the finite skin thickness case to the simulation which assumes a homogeneous skin half-space, the observed time of the first reflection yields information for the skin thickness. 2-D FDTD simulations were run to obtain the all-skin response and responses for assumed skin thicknesses of 0.6, 1.2, 1.8 and 2.4mm. Then, the estimated time of the peak value of the first reflection with respect to the peak of the all-skin response is used to estimate the skin thickness (Fig. 2). The resulting breast skin thickness values obtained in this manner were 0.51, 1.25, 1.85 and 2.45mm.

2.4 Time-domain inverse-scattering scheme: obtaining $\varepsilon_{r\text{-}skin}$ and σ_{skin} from the received signal

This section summarizes continuing work on a 2-D FDTD inverse-scattering technique for obtaining skin relative permittivity $\varepsilon_{r\text{-}skin}$ and electric conductivity σ_{skin}. The algorithm is based on a previously reported work on one-dimensional "layer stripping" [4]. An antenna adjacent to the skin emits a sub-nanosecond pulse. The antenna also acts as a receiver to collect the backscattered signal. The time evolution of the backscattered signal contains information on tissue layers located progressively deeper within the breast. We begin the inverse-scattering algorithm by making an intelligent guess for the unknown skin properties. These parameters are fed into an FDTD forward-scattering element, which calculates a trial backscattered signal. The trial and measured backscattered signals are then compared and used to establish an error value. If error criteria are not met, the values of $\varepsilon_{r\text{-}skin}$, σ_{skin} are perturbed using a gradient-search method to yield another trial set of parameters and another backscattered signal, which is again compared to the reference signal. This procedure is repeated until the values of $\varepsilon_{r\text{-}skin}$ and σ_{skin} used in the FDTD simulation yield a calculated backscattered response sufficiently close to the measured backscattered signal. In the previous Annual Report [5], we illustrated convergence

of $\varepsilon_{r\text{-}skin}$ for two initial guesses of $\varepsilon_{r\text{-}skin}$ and σ_{skin} being fixed to its nominal value. Similar convergence was shown for σ_{skin} with $\varepsilon_{r\text{-}skin}$ fixed.

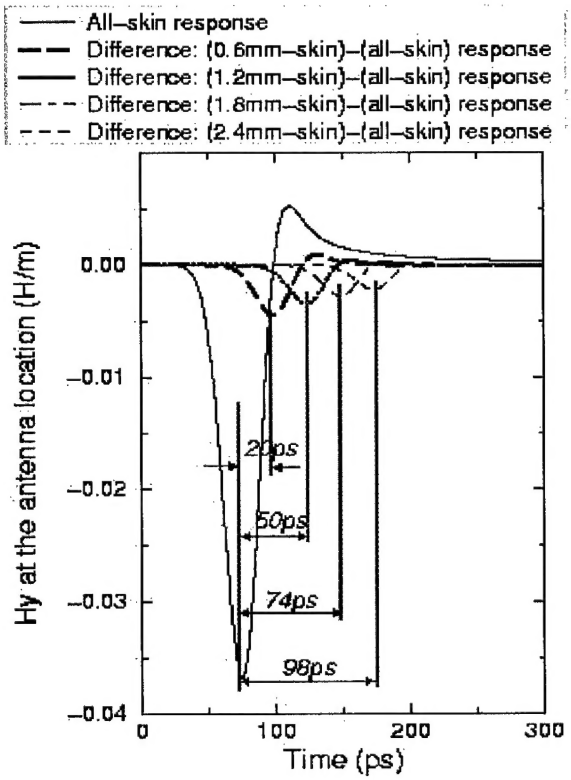

Figure 2. Estimate of skin thickness with previously determined $\varepsilon_{r\text{-}skin}$, σ_{skin} . We compare the peak response (magnetic field component at the location of the antenna) for the finite skin thickness case to the simulation which assumes a homogeneous skin half-space. The observed time of the first peak reflection yields information for the skin thickness. Signal used in the shown study is a 60-ps differentiated Gaussian pulse.

For the study of search trajectory in the ($\varepsilon_{r\text{-}skin}$, σ_{skin}) space, we considered several incident waveforms and durations. Here, we summarize the methodology of investigation by presenting our findings for three excitation waveforms: a 120-ps differentiated Gaussian pulse, a 5-ps differentiated Gaussian pulse, and a 5-ps rise-time ramp function, having an amplitude equal to that of the 5-ps differentiated Gaussian. In each case, the skin thickness was fixed to 1 mm. For each signal waveform under consideration, we implement the following steps in our analysis:

Step 1. Use FDTD to calculate a simulated measured response for a 1-mm-thick skin layer adjacent to a breast tissue half-space, assuming literature values, $\varepsilon_{r\text{-}skin}$=36 and σ_{skin} = 4 S/m. Estimate the time window for pulse T_{window} for the inverse-scattering operations to avoid reflections from the underlying breast-skin interface.

Step 2. For each $\varepsilon_{r\text{-}skin}$ in the range of 50% around the nominal value, run the inverse-scattering code for T_{window} . This iteratively estimates σ_{skin} until the imposed error criterion is met. Therefore, for each assumed $\varepsilon_{r\text{-}skin}$, the code converges to a corresponding value of σ_{skin} . The calculated set of values for the whole range of $\varepsilon_{r\text{-}skin}$ under investigation yields a search trajectory in the ($\varepsilon_{r\text{-}skin}$, σ_{skin}) parameter space, as shown in Fig. 3(a), Fig. 4(a) and Fig. 5(a). This trajectory should include, with an allowed small deviation, the point of nominal values, $\varepsilon_{r\text{-}skin}$=36 and σ_{skin} = 4 S/m.

Step 3. For each estimated σ_{skin} obtained in the previous step, we plot the cumulative error, i.e. the difference between the trial signal and the simulated measured signal for all time steps

within T_{window} in the L_2-normed sense. Sample curves of error vs. σ_{skin} are graphed in Fig. 3(b), Fig. 4(b) and Fig. 5(b). In each graph, the minimum error occurs for the value closest to the reference value, σ_{skin} = 4 S/m. This implies that minimizing the L_2-normed error can be used as the search criterion along the determined trajectory in the ($\varepsilon_{r\text{-}skin}$, σ_{skin}) parameter space to reach the assumed reference point.

Several key conclusions can be drawn from Fig. 3, 4 and 5. First, T_{window} must be carefully chosen. It is critical that T_{window} be small enough to avoid the reflection from the skin-breast interface, which corrupts the received signal. However, T_{window} must be large enough to allow the received pulse to contain meaningful information concerning the skin electrical parameters. Second, the shape of the search trajectory in the ($\varepsilon_{r\text{-}skin}$, σ_{skin}) space and the cumulative error function depends on the time waveform of the excitation signal and its duration. In Fig. 3(a), for the 120-ps differentiated Gaussian pulse, T_{window} = 400 time steps. This period covers only the leading edge of the pulse, and the trajectory in the ($\varepsilon_{r\text{-}skin}$,σ_{skin}) space is a straight line. In Fig. 4(a), for the 5-ps differentiated Gaussian response, T_{window} = 80 time steps. This period covers the complete pulse, and the trajectory in the the ($\varepsilon_{r\text{-}skin}$, σ_{skin}) space is a parabolic function. Linearity of the search trajectory is again observed for the 5-ps ramp function. We note that the cumulative L_2-normed error function has a much sharper minimum in Fig. 4(b) than either in Fig. 3(b) and Fig. 5(b). This is favorable for accurate skin parameter determination in the presence of noise, which will be studied in the near-future work.

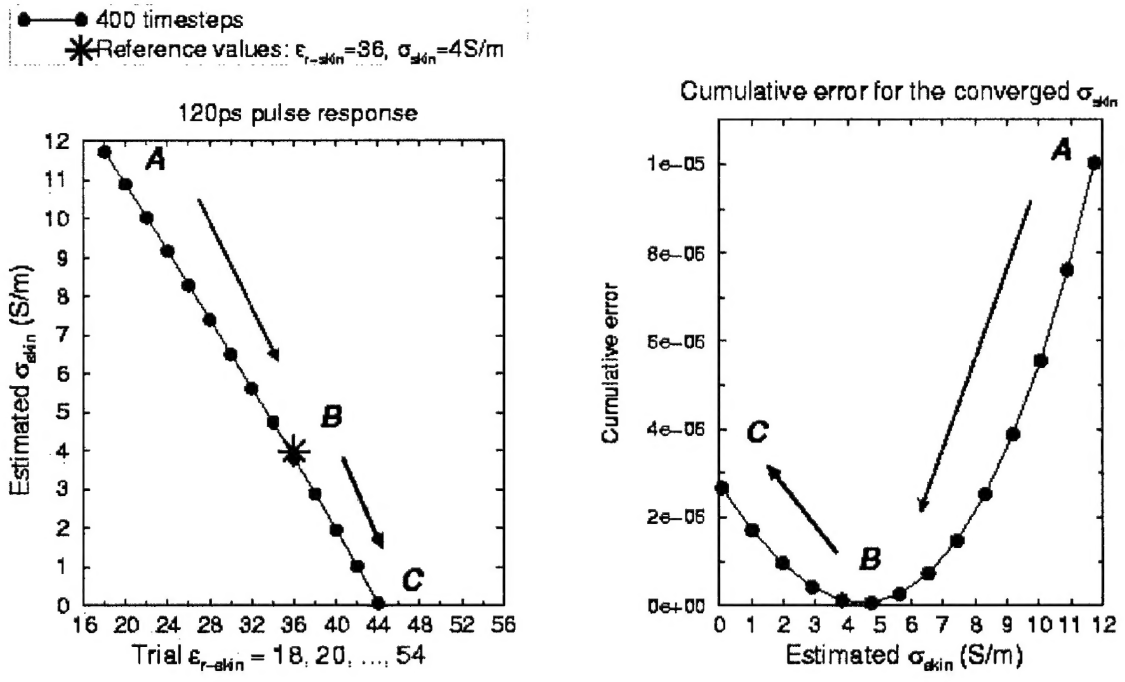

(a) (b)

Figure 3. Results for the 120-ps differentiated Gaussian pulse excitation. (a) Search trajectory in ($\varepsilon_{r\text{-}skin}$, σ_{skin}) space search. T_{window} = 400 time steps , where Δt=0.3335ps. (b) The cumulative error vs. estimated σ_{skin} values, showing a broad null at the location of the assumed accurate values of the skin parameters.

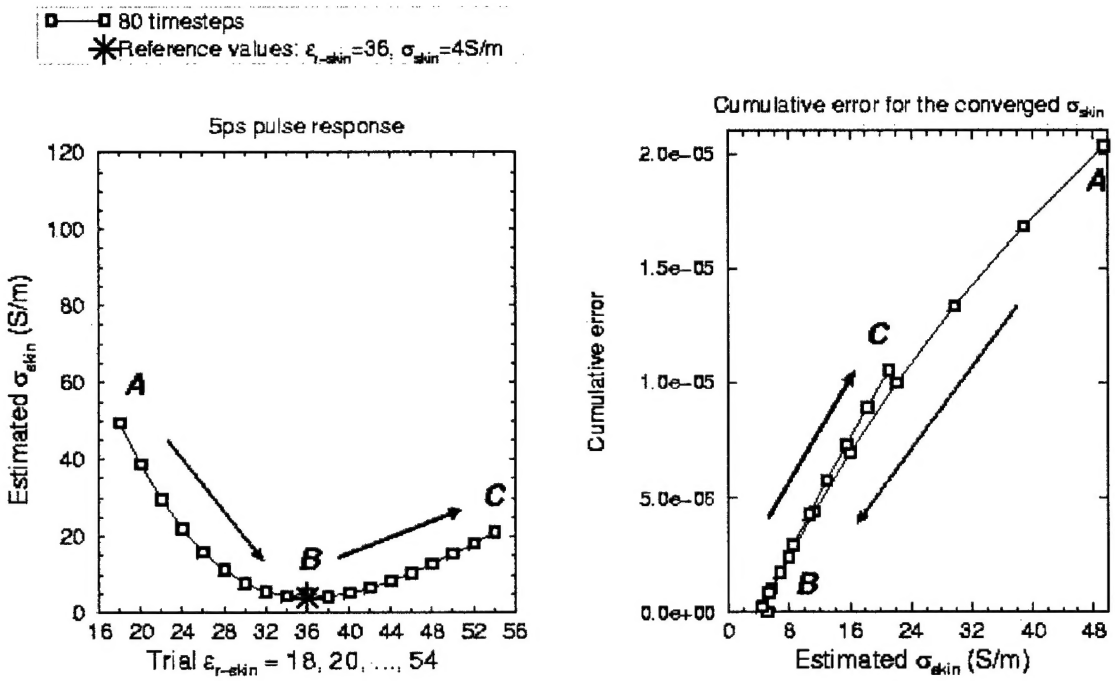

(a) (b)

Figure 4. Results for the 5-ps differentiated Gaussian pulse excitation. (a) Search trajectory in ($\varepsilon_{r\text{-}skin}$, σ_{skin}) space. T_{window} = 80 time steps , where Δt=0.3335ps. (b) The cumulative error vs. estimated σ_{skin} values, showing a sharp null at the location of the assumed accurate values of the skin parameters.

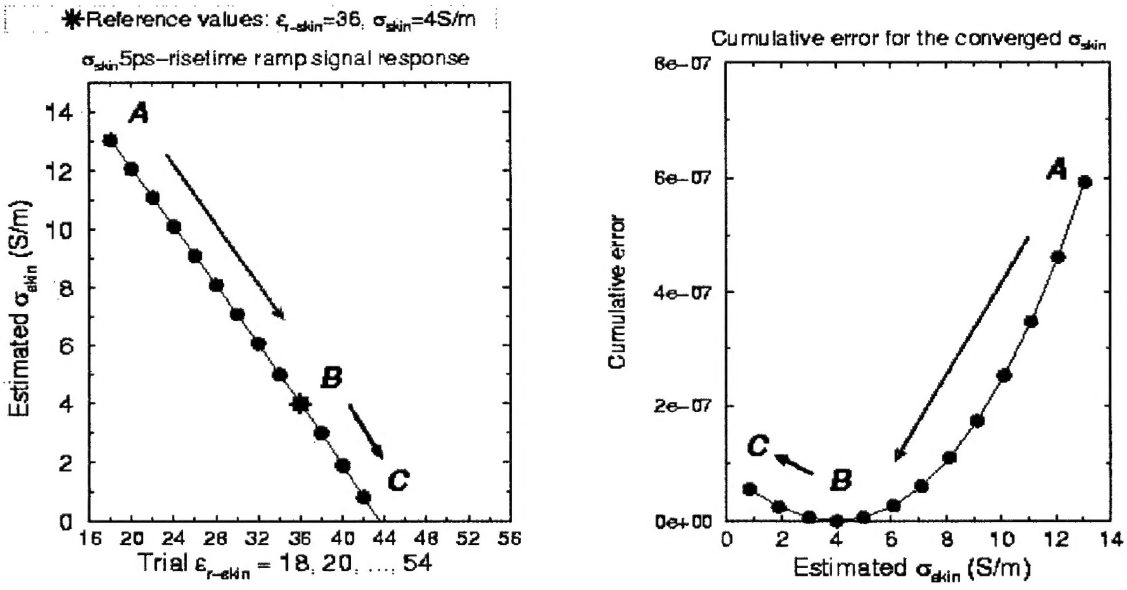

(a) (b)

Figure 5. Results for the 5-ps risetime ramp signal excitation. The amplitude of the excitation is the same as the maximal value of the 5-ps differentiated Gaussian with results in Fig. 4. (a) Search trajectory in ($\varepsilon_{r\text{-}skin}$, σ_{skin}) space. T_{window} = 100 time steps , where Δt=0.3335ps. (b) The cumulative error vs. estimated σ_{skin} value, showing a broad null at the location of the assumed accurate values of the skin parameters.

3. Key Research Accomplishments

- Thorough study of the skin within the area of human breast (normal thickness range, abnormalities, causes of thickening).

- Analysis of importance of determining accurate, local, patient-specific breast thickness in calibration of the microwave detection and imaging system.

- 2-D development of an inverse-scattering FDTD algorithm for simultaneous recovery of electrical parameters of the skin (relative permittivity $\varepsilon_{r\text{-}skin}$ and electrical conductivity σ_{skin}) from a simulated backscattered signal:
  - Locating search trajectory in the ($\varepsilon_{r\text{-}skin}$, σ_{skin}) space ;
  - Determining the L2-normed error along the search trajectory ;
  - Determining search trajectory dependence on the shape and duration of the excitation signal waveform, then optimizing.

- Principle for determining skin thickness after the recovery of $\varepsilon_{r\text{-}skin}$ and σ_{skin} .

- Current work: testing the robustness of the 2-D FDTD inverse-scattering algorithm in the presence of Gaussian noise .

4. Reportable Outcomes

Conference papers and presentations: (please see appendices)

[Appendix A] M. Popovic and A. Taflove, "Obtaining Microwave Properties of Near-Surface Body Tissues Using 2-D FDTD Inverse-Scattering Technique", The Bioelectromagnetics Society (BEMS), Twenty-Second Annual Meeting Abstract Book, The Technical University, Munich, Germany, June 11-16, 2000, pp. 23-24.

[Appendix B] M. Popovic and A. Taflove, "Time Domain Inverse-Scattering Technique for Obtaining Microwave Properties of Near-Surface Body Tissues", Progress In Electromagnetics Research Symposium (PIERS) 2000, Proceedings, Cambridge, Massachusetts, USA, July 5-14, 2000, pp. 550.

[Appendix C] M. Popovic and A. Taflove, "Skin Thickness and Dielectric Parameter Evaluation in the Microwave Range Using and FDTD Inverse-Scattering Technique", 2001 URSI International Symposium on Electromagnetic Theory, Proceedings, Victoria, Canada, May 13-17, 2001, pp. 482-484.

Awards:

EMF Clinical Applications Award, The Bioelectromagnetics Society (BEMS), Twenty-Second Annual Meeting Abstract Book, The Technical University, Munich, Germany, June 11-16, 2000.

5. Conclusions

Motivated by the need to calibrate the recently proposed microwave breast tumor detection system, we are investigating a two-dimensional time-domain inverse-scattering algorithm for determining skin thickness, electrical permittivity $\varepsilon_{r\text{-}skin}$ and conductivity σ_{skin}.

Skin thickness within the human breast exhibits patient-to-patient and regional anatomical variations. Simple analysis of the 2-D geometry used to study image-formation signal processing algorithm of the microwave breast cancer detection system shows that the knowledge of the correct value for skin thickness is essential for accurate operation of the system. In addition to helping calibrate such a system, a non-invasive means of calculating local breast skin thickness from the information contained in the backscattered signals may serve as a pre-diagnostic tool for possible underlying disease in the breast and the human body in general.

We conducted a study of a novel two-dimensional time-domain inverse-scattering algorithm for simultaneous estimate of electrical parameters of the skin ($\varepsilon_{r\text{-}skin}$ and σ_{skin}). This algorithm traces a search trajectory in the ($\varepsilon_{r\text{-}skin}$, σ_{skin}) space. The minimal parameter estimation error along this trajectory yields a set of correct parameter values. These results of the inverse-scattering technique depend on the shape and the duration of the pulse chosen for the electrical parameter reconstruction.

The time-domain nature of the inverse-algorithm allows for limiting the region of inversion. Thus, when the parameters of skin are estimated, the skin thickness can be determined by comparing the measurement with a simulated all-skin response.

Current and near-future work involves testing the algorithm robustness in the presence of Gaussian noise for various signal-to-noise ratios. The following logical step is the expansion of the method to include recovery of electrical parameters of the underlying tissue layer.

REFERENCES

[1] S. C. Hagness, A. Taflove and J.E. Bridges, "Two-Dimensional FDTD Analysis of a Pulsed Microwave Confocal System for Breast Cancer Detection: Fixed-Focus and Antenna-Array Sensors", *IEEE Trans. Biomedical Eng.*,vol. 45, no. 12, Dec. 1998, pp. 1470-1479.

[2] E. C. Fear and M. A. Stuchly, "Microwave Detection of Breast Cancer", *IEEE Trans. Microwave Theory and Techniques,* vol 48, no. 11, Nov. 2000, pp. 1470-1479.

[3] Jr. T. L. Pope, M. E. Read, T. Medsker, A. J.. Buschi and A. N. Brenbridge, "Breast skin thickness: normal range and causes of thickening shown on film-screen mammography", *J. Canadian Assoc. of Radiologists,* vol. 35, Dec. 1984, pp. 365-693.

[4] K. R. Umashankar, S. Chaudhuri and A. Taflove, "Finite-difference time-domain formulation of an inverse-scattering scheme for remote sensing of inhomogeneous lossy layered media", *J. Electromagn. Waves Apps.*, vol. 8, pp. 489-509, 1994.

[5] M. Popovic and A. Taflove, Annual Report May 2000, NTIS, document reference number: AD385306.

[6] A. S. Breathnach, *An Atlas of the Ultrastructure of Human Skin*, J. & A. Churchill, London, 1971.

[7] R. M. Marks, S. P. Barton and C. Edwards, eds., *The Physical Nature of the Skin*, MTP Press Ltd, Lancaster, England,1988. pp. 2271-2293.

[8] D. Gilligan, J. A. Hendry and J. R. Yarnold, "The use of ultrasound to measure breast thickness to select electron energies for breast boost therapy", *Radiotherapy and Oncology*, Vol. 32, 1994. pp 265-273.

[9] J. P. Grant, R. N. Clarke, G. T. Symm and N. M Spyrou, "*In vivo* dielectric properties of human skin from 50 MHz to 2.0 GHz", *Physics in Medicine and Biology*, Vol. 33, No. 5, 1998, pp. 607-612.

[10] H. I. Libshitz, E. D. Montague and D. D. Paulus, Jr.,"Skin thickness in the therapeutically irradiated breast", *American Journal of Roentgenology*, Vol. 130, 1978, pp. 345-347.

[11] G. T. Mogavero, E. K. Fishman and J. E. Kuhlman, "Inflammatory breast cancer: {CT} evaluation", *Clinical Imaging*, Vol. 16, 1992, pp. 183-186.

[12] M. Olenius and O. Johansson, "Variations in epidermal thickness in expanded human breast skin", *Scandinavian Journal of Plastic and Reconstructive and Hand Surgery*, Vol. 29, 1995, pp. 15-20.

[13] D. Sulitzeanu, "Markers in breast cancer", *Israel Journal of Medical Science*, 1981, pp. 865-868.

[14] T. Tamura, M. Tenhunen, T. Lahtinen and H. P. Schwan, "Modelling of the dielectric properties of normal and irradiated skin", *Physics in Medicine and Biology*, Vol. 39, 1994, pp. 927-936.

[15] S. A. Wilson and E. J. Adam and A. K. Tucker, "Patterns of breast skin thickness in normal mammograms", *Clinical Radiology*, Vol. 33, 1982, pp. 691-693.

APPENDIX A: The Bioelectromagnetics Society (BEMS), Twenty-Second Annual Meeting Abstract Book, The Technical University, Munich, Germany, June 11-16, 2000, pp. 23-24.

OBTAINING MICROWAVE PROPERTIES OF NEAR-SURFACE BODY TISSUES USING 2-D FDTD INVERSE-SCATTERING TECHNIQUE. M. Popovic and A. Taflove*, Northwestern University, Evanston, Illinois 60208, USA.

OBJECTIVE: Our goal is to demonstrate a 2-D FDTD inverse-scattering algorithm that, when extemded to 3-D, will permit a noninvasive measurement of microwave properties of the near-surface body tissues. METHOD: We use the measured "early-time" response of an ultrawide-band sensor element to unfold the dielectric properties and thickness of the skin and the average dielectric properties of the tissue beneath the skin. The measured data are time samples of $Z(t)$, the ratio of the voltage and current waveforms observed at the driving point of the element. We analyze the $Z(t)$ data by adapting the technique reported (Umashankar *et al.*, *J. Electromagn. Waves Apps.*, 1994) for unfolding the properties of a layered half-space from plane-wave pulse-reflection measurements taken at its surface. Here, an initial guess for the layer thicknesses and dielectric parameters is provided to an FDTD forward-scattering code which calculates the reflected pulse at the surface. This pulse is subtracted from the measured response to yield an error signal that is provided to a Levenberg-Marquardt (LM) nonlinear optimization routine. Based upon the norm of the error signal, the LM routine generates an improved guess for the layer thicknesses and dielectric parameters. This improved guess is fed back to the FDTD forward-scattering code which calculates a new reflected pulse at the surface and the process repeats. Convergence occurs when no further reduction of the error signal is possible. At this point, the final layer thicknesses and electrical properties used in the FDTD element are taken to be parameters of the physical system. In the present problem, the excitation is not a normally incident plane wave. Instead, it is an approximately spherical wave originating at the feedpoint of the antenna element. The method reported in the literature must therefore be adapted. In this initial work, we implement this change by substituting a 2-D forward-scattering FDTD code for the 1-D forward-scattering FDTD code. Representative numerical simulations are provided that include the effects of simulated additive Gaussian noise. RESULTS: We have found that a 2-D FDTD inverse-scattering algorithm yields accurate data for skin thickness, skin dielectric properties and the dielectric properties of the tissues immediately under the skin in the presence of the additive Gaussian noise. DISCUSSION: The proposed technique may assist the development of recently reported noninvasive microwave imaging schemes utilizing the backscatter of short pulses. Such methods require a good estimate of the average skin thickness and properties of the underlying tissues to unfold the impulsive backscattered waveform, thereby obtaining an image of subcutaneous tissues. This work was supported by United States Department of Defense Pre-doctoral Traineeship BC981143.

APENDIX B: Progress In Electromagnetics Research Symposium (PIERS) 2000, Proceedings, Cambridge, Massachusetts, USA, July 5-14, 2000, pp. 550.

Time Domain Inverse Scattering Technique for Obtaining Microwave Properties of Near-Surface Body Tissues

Milica Popovic and Allen Taflove

This paper reports a time-domain inverse-scattering algorithm that permits a noninvasive measurement of microwave properties of the near-surface body tissues. We use the measured "early-time" response of an ultrawide-band sensor element to unfold the dielectric properties and thickness of the skin and the average dielectric properties of the tissue beneath the skin. The measured data are time samples of $Z(t)$, the ratio of the voltage and current waveforms observed at the driving point of each element.

We analyze the $Z(t)$ data by adapting the technique reported in [1] for unfolding the properties of a layered half-space from plane-wave pulse-reflection measurements taken at its surface. Here, an initial guess for the layer thicknesses and dielectric parameters is provided to an FDTD forward-scattering code which calculates the reflected pulse at the surface. This pulse is subtracted from the measured response to yield an error signal that is provided to a Levenberg-Marquardt (LM) nonlinear optimization routine. Based upon the norm of the error signal, the LM routine generates an improved guess for the layer thicknesses and dielectric parameters. This improved guess is fed back to the FDTD element which calculates a new reflected pulse at the surface and the process repeats. Convergence occurs when no further reduction of the error signal is possible. At this point, the final layer thicknesses and electrical properties used in the FDTD element are taken to be parameters of the physical system.

In the present problem, the excitation is not a normally incident plane wave. Instead, it is an approximately spherical wave originating at the feedpoint of the antenna element. The method of [1] must therefore be adapted. In this initial work, we implement this change by substituting a 2-D forward-scattering FDTD code for the 1-D forward-scattering FDTD code reported in [1]. Representative numerical simulations are provided that include the effects of simulated additive Gaussian noise.

The proposed technique may assist the development of recently reported noninvasive microwave imaging schemes utilizing the backscatter of short pulses. Such methods require a good estimate of the average skin thickness and properties of the underlying tissues to unfold the impulsive backscattered waveform, thereby obtaining an image of subcutaneous tissues.

Reference

[1] K. R. Umashankar *et al.*, *J. Electromagn. Waves Apps.*, vol. 8, pp. 489-509, 1994.

Topic category: ***1. Electromagnetic theory, diffraction, scattering and inverse scattering***
Preferred presentation: ***platform***

APPENDIX C: 2001 URSI International Symposium on Electromagnetic Theory, Proceedings, Victoria, Canada, May 13-17, 2001, pp. 482-484.

SKIN THICKNESS AND DIELECTRIC PARAMETER EVALUATION IN THE MICROWAVE RANGE USING AN FDTD INVERSE-SCATTERING TECHNIQUE

M. Popovic, A. Taflove
Electrical and Computer Eng. Dept., Northwestern University, Evanston, Illinois 60208, USA

Abstract. We are investigating a time-domain inverse-scattering technique to measure the skin thickness and dielectric parameters in the area of the human breast. Our study is motivated by several well-documented findings. Accurate values of breast skin thickness and dielectric parameters would help to perform patient-specific calibration of a recently proposed microwave detection system for breast tumors [1],[2]. Furthermore, skin thickness can be used to assist the diagnosis of possible underlying tissue disease [3].

Skin thickness in the area of the human breast. Breast skin thickness can be estimated from film-screen mammograms [3]. Skin thickness is patient-specific, but we also note that within a single patient measurements revealed regional anatomical variations. From the mediolateral view, the range in skin thickness in the superior breast area is 0.7-2.3mm, and in the inferior area 0.7-2.7mm. From the craniocaudad view, skin thickness ranges 0.6-2.4mm and 0.5-2.1mm in the medial and lateral area, respectively. A number of factors can cause thickening of mammary skin [3]. The major reported localized causes are carcinoma, inflammation, trauma, fat necrosis, post-biopsy and dermatological conditions. Among the generalized factors associated with increase in breast skin thickness are breast cancer, metastatic disease, inflammation, primary skin disorders, anasarca, any cause of lymphatic obstruction, radiation therapy and surgery. Although our study is primarily motivated by assisting patient-specific calibration of the microwave breast cancer imaging system of [1,2], we note that determining breast skin thickness can also help diagnose possible pathologies in the underlying tissue and in the patient in general.

Microwave breast tumor imaging system and its dependency on the correct skin thickness. To illustrate the importance of knowledge of correct skin thickness value on the operation of the microwave tumor imaging system of [1] in Fig. 1(a) we sketch a simplified 2-D geometry of a 17-element microwave antenna array system adjacent to the breast skin. Beneath the skin is a homogeneous slab of the fatty breast tissue. We assume the tumor location to be on the antenna array axis and 3 cm deep in the breast tissue. The system relies on high dielectric contrast between tumors and the healthy tissue in the microwave frequency range (relative electric permittivity: tumor $\varepsilon_{r\text{-}tumor} = 50$, breast tissue $\varepsilon_{r\text{-}breast} = 9$, skin $\varepsilon_{r\text{-}skin} = 36$, electric conductivity: tumor $\sigma_{tumor} = 7$ S/m, breast tissue $\sigma_{breast} = 0.4$ S/m, skin $\sigma_{skin} = 4$ S/m) [1]. A sub-nanosecond pulse is launched from each array element, which then collects the reflection. For each element, there is a time delay between the pulse transmission and its received reflection. This delay is determined by a propagation path illustrated in Fig. 1(a), and calculated with assumed knowledge of skin thickness and dielectric parameters of skin and breast tissue – all media present in the propagation path. As a signal processing stage, the difference in time delays for different array elements is used to shift and coherently sum signals received by individual elements, thus achieving signal gain through this coherent summation. Therefore, an incorrect assumption of skin thickness and/or $\varepsilon_{r\text{-}skin}$ can cause incorrect calculation of time delays and hence lack of coherency in summation of signals received by different antenna array elements. Fig. 1(b) graphs the calculated time delays as a function of antenna element location for the extreme values of the breast skin thickness range. We see that the variation in these delays for two skin thickness values is comparable to the difference in time delays for two adjacent antennas for each thickness value under consideration. We conclude that the knowledge of the correct value for skin thickness at each point of the imaged breast area is essential for efficient operation of the newly proposed microwave breast cancer detection system.

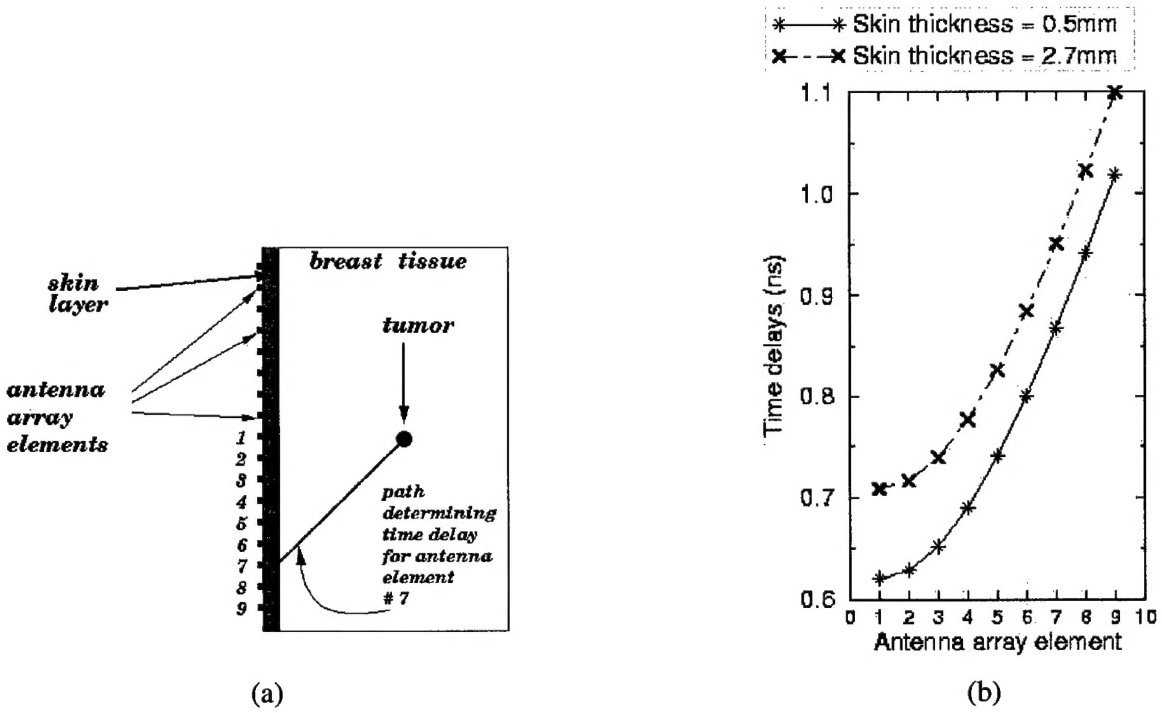

Figure 1. (a) 2-D sketch of the microwave antenna array used for breast tumor detection. The sketch shows the propagation path used to determine time delay between transmission and reception of the signal backscattered from the tumor for each antenna element. (b) Analytically calculated time delays for antenna array elements for extreme values of the reported breast skin thickness range.

Time-domain inverse-scattering scheme: obtaining $\varepsilon_{r\text{-}skin}$ and σ_{skin} from the received signal. In this paper, we summarize the basis of a 2-D FDTD inverse-scattering technique for obtaining skin parameters. The technique has previously been studied for a 1-D layered medium illuminated by a plane wave [4]. We assume that the following skin properties are of interest and thus represent three unknown variables: relative electric permittivity $\varepsilon_{r\text{-}skin}$, electric conductivity σ_{skin}, and skin thickness.

An antenna adjacent to the skin emits a sub-nanosecond pulse. The antenna also acts as a receiver to collect the backscattered signal. The time evolution of the backscattered signal contains information on tissue layers located progressively deeper within the breast. We begin the inverse-scattering algorithm by making an intelligent guess for the unknown skin properties. These parameters are fed into an FDTD forward-scattering element, which calculates a trial backscattered signal. The trial and measured backscattered signals are then compared and used to establish an error value. If error criteria are not met, the values of $\varepsilon_{r\text{-}skin}$, σ_{skin} are perturbed using a gradient-search method to yield another trial set of parameters and another backscattered signal, which is again compared to the reference signal. This procedure is repeated until the values of $\varepsilon_{r\text{-}skin}$ and σ_{skin} used in the FDTD simulation yield a calculated backscattered response sufficiently close to the measured backscattered signal. Fig. 2(a) illustrates convergence of $\varepsilon_{r\text{-}skin}$ for two initial guesses of $\varepsilon_{r\text{-}skin}$ and σ_{skin} being fixed to its nominal value. Similar convergence is observed for σ_{skin} with $\varepsilon_{r\text{-}skin}$ fixed.

Once the patient-specific values for $\varepsilon_{r\text{-}skin}$ and σ_{skin} are determined, we can proceed with a simpler algorithm to determine the breast skin thickness, as illustrated with FDTD simulation results in Figure 2(b). Due to the dielectric contrast between skin and the underlying breast tissue, the propagating pulse reflects off the skin – breast tissue interface. By comparing the response for the finite skin thickness case to the simulation which assumes a homogeneous skin half-space, the observed time of the first reflection yields information for the skin thickness. 2-D FDTD simulations were run to obtain the all-skin response and responses for assumed skin thicknesses of 0.6, 1.2, 1.8 and 2.4mm. Then, the estimated time of the peak value of the first reflection with

respect to the peak of the all-skin response is used to estimate the skin thickness (Fig. 2(b)). The resulting breast skin thickness values obtained in this manner were 0.51, 1.25, 1.85 and 2.45mm.

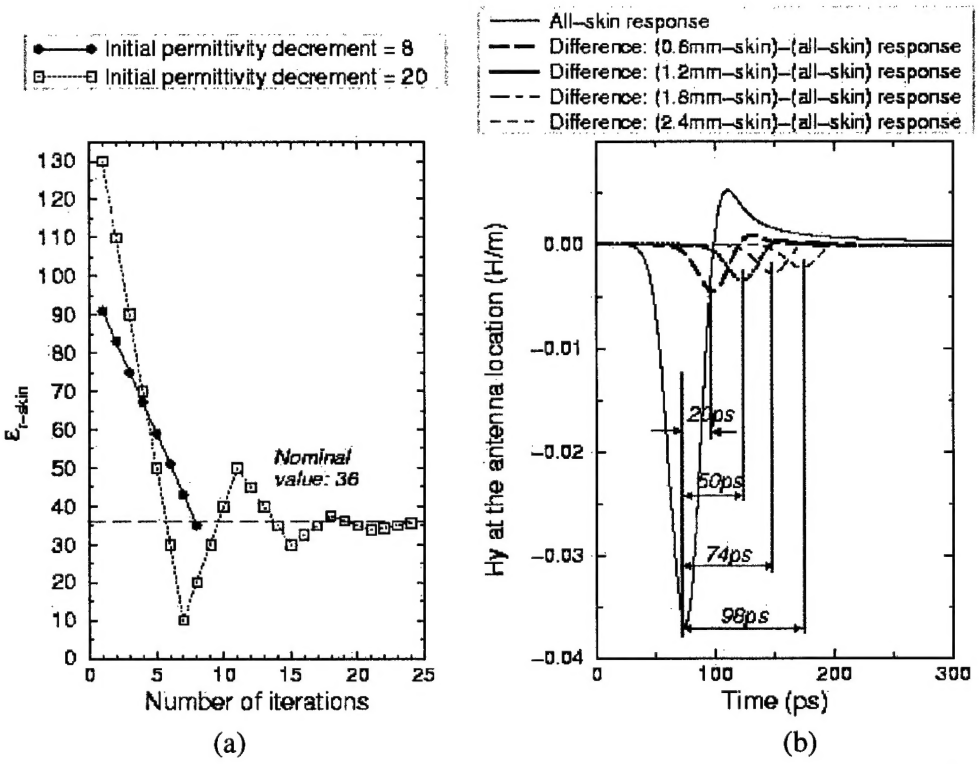

Figure 1. (a) Convergence of $\varepsilon_{r\text{-}skin}$ obtained by the FDTD inverse-scattering scheme for a fixed value of σ_{skin}=4S/m. (b) Estimate of skin thickness with previously determined $\varepsilon_{r\text{-}skin}$, σ_{skin} . We compare the peak response for the finite skin thickness case to the simulation which assumes a homogeneous skin half-space. The observed time of the first peak reflection yields information for the skin thickness. Signal used in the shown study is a 60-ps differentiated Gaussian pulse.

Near-future work and acknowledgements. Current investigations involve algorithms which determine $\varepsilon_{r\text{-}skin}$, σ_{skin} and skin thickness simultaneously. Subsequently, the methodology for recovering dielectric skin parameters can be used for simultaneous calculation of the underlying breast tissue properties, $\varepsilon_{r\text{-}breast}$ and σ_{breast} . This work is funded by United States Department of Defense Pre-Doctoral Grant (Award Number: DAMD17-99-1-9335).

REFERENCES

[1] S. C. Hagness, A. Taflove and J.E. Bridges, "Two-Dimensional FDTD Analysis of a Pulsed Microwave Confocal System for Breast Cancer Detection: Fixed-Focus and Antenna-Array Sensors", *IEEE Trans. Biomedical Eng.*,vol. 45, no. 12, Dec. 1998, pp. 1470-1479.

[2] E. C. Fear and M. A. Stuchly, "Microwave Detection of Breast Cancer", *IEEE Trans. Microwave Theory and Techniques,* vol 48, no. 11, Nov. 2000, pp. 1470-1479.

[3] Jr. T. L. Pope, M. E. Read, T. Medsker, A. J.. Buschi and A. N. Brenbridge, "Breast skin thickness: normal range and causes of thickening shown on film-screen mammography", *J. Canadian Assoc. of Radiologists,* vol. 35, Dec. 1984, pp. 365-693.

[7] K. R. Umashankar, S. Chaudhuri and A. Taflove, "Finite-difference time-domain formulation of an inverse-scattering scheme for remote sensing of inhomogeneous lossy layered media", *J. Electromagn. Waves Apps.*, vol. 8, pp. 489-509, 1994.